Photocatalytic Activities of Porous Titania and Titania/Zirconia Structures Formed by Using a Polymer Gel Templating Technique

Jan H. Schattka, Dmitry G. Shchukin, Jianguang Jia, Markus Antonietti, and Rachel A. Caruso*

Max Planck Institute of Colloids and Interfaces, D-14424 Potsdam, Germany

Received June 18, 2002. Revised Manuscript Received September 20, 2002

The formation of porous metal oxide networks using mixed titania/zirconia precursor solutions was achieved by a polymer gel templating technique. The inorganic porous materials result from a coating of the initial template with obvious structural similarities between the polymer gel and the final inorganic network. The mixed TiO_2/ZrO_2 network structures exhibit higher surface areas than a corresponding pure titania network, and in a certain range of metal oxide compositions X-ray amorphous mixed glasses are obtained upon calcination at 500 °C. The photocatalytic efficiencies of the TiO_2 and TiO_2/ZrO_2 networks have been assessed by monitoring the photodecomposition of two organic molecules: salicylic acid and 2-chlorophenol. The TiO_2 network was found to exhibit an efficiency of ≈60% and ≈65% of the standard Degussa P25 TiO_2 (of nanoparticulate morphology) for the salicylic acid and 2-chlorophenol reactions, respectively. For both photocatalytic reactions the presence of zirconia in the titania network (at a molar ratio of 1:9) resulted in enhanced photocatalytic activity relative to the pure TiO_2 network (80% and 100% the efficiency of Degussa P25), which is believed to be due to a number of factors including an increased surface area and a decrease of the anatase to rutile crystal phase transformation. A further increase in the zirconia-to-titania ratio leads to decreased activity as amorphous materials are obtained and zirconia itself does not act as a photocatalyst under the experimental conditions used.

Introduction

Morphological control or morphosynthesis of materials involves regulation of the overall outer structure, shape and size, as well as inner structure, pore size and connectivity, the colloidal dimensions, and—in the case of potential polymorphs—also the crystal phase of the components making up the object. Novel inorganic networks with controlled morphology and properties can be fabricated using templating procedures.[1] Organic materials have numerous structures and forms which can be regulated (in terms of dimension, structural density, etc.) and they can be readily removed using heating processes; hence, they are frequently applied as templates for the formation of inorganic structures. Examples of the use of organic templates include (i) the creation of mesoporous silica materials with tuneable pore structures from block copolymers and surfactants,[2] (ii) the use of latices, for which variable diameters are obtainable, to fabricate hollow spheres with diameters that can be regulated[3] and macroporous structures[4] with tailorable pore sizes, and (iii) the utilization of membranes and polymer gels that can be produced with different pore structures and densities for the construction of inorganic films[5,6] and monolithic conformations[7] containing macropores.

Inorganic materials produced by this mode of material molding will have advantages in areas of application where high porosities and large specific surface, plus adsorption and surface mediated reactions are key factors.

One such application for substances with these characteristics is photocatalysis. Photochemical degradation can be used for the decomposition of toxic organic contaminants in wastewater.[8] This process involves the absorption of light by a semiconductor, forming electron and hole pairs, which can lead to oxidation and reduction reactions. Many organic and some inorganic compounds are degraded in aqueous dispersions of TiO_2 under illumination with UV light.[9] Morphosynthesis of a TiO_2 material with ideal properties for a photocatalytic device requires monolithic structure (to avoid tedious

* To whom correspondence should be addressed. Fax: +49 331 567 9502. E-mail: Rachel.Caruso@mpikg-golm.mpg.de.

(1) Caruso, R. A.; Antonietti, M. *Chem. Mater.* **2001**, *13*, 3272−3283.
(2) See for example: (a) Zhao D.; Feng, J.; Huo, Q.; Melosh, N.; Fredrickson, G. H.; Chmelka, B. F.; Stucky, G. D. *Science* **1998**, *279*, 548−552. (b) Göltner, C. G.; Berton, B.; Krämer, E.; Antonietti, M. *Chem. Commun.* **1998**, 2287−2288. (c) Smarsly, B.; Polarz, S.; Antonietti, M. *J. Phys. Chem. B* **2001**, *105*, 10473−10483. (d) Kim, J. M.; Sakamoto, Y.; Hwang, Y. K.; Kwon, Y.-U.; Terasaki, O.; Park, S.-E.; Stucky, G. D. *J. Phys. Chem. B* **2002**, *106*, 2552−2558.
(3) Caruso, R. A.; Susha, A.; Caruso, F. *Chem. Mater.* **2001**, *13*, 400−409.
(4) For a review see Stein, A. *Microporous Mesoporous Mater.* **2001**, *44*−*45*, 227−239.
(5) Martin, C. R. *Chem. Mater.* **1996**, *8*, 1739−1746.
(6) Caruso, R. A.; Schattka, J. H. *Adv. Mater.* **2000**, *12*, 1921−1923.
(7) Caruso, R. A.; Giersig, M.; Willig, F.; Antonietti, M. *Langmuir* **1998**, *14*, 6333−6336.
(8) Mills, A.; Le Hunte, S. *J. Photochem. Photobiol. A: Chem.* **1997**, *108*, 1−35.
(9) Legrini, O.; Oliveros, E.; Braun, A. M. *Chem. Rev.* **1993**, *93*, 671−698.

10.1021/cm021238k CCC: $22.00
Published on Web 11/22/2002

removal or leaching of the catalyst), a high surface area on which the heterogeneous surface catalysis reaction occurs, and enhanced porosity with rational pore connectivity to optimize the flow rate through the catalyst.

Another means of improving the catalytic efficiency of metal oxides and their application as support materials for catalysis is to dope the metal oxide with a metal or to combine it with another metal oxide.[10,11] Examples of mixed oxides include the combination of TiO_2 with SiO_2, ZrO_2, or Al_2O_3.[12−16] These combined metal oxide materials result in new reactivity properties and higher activity when compared with the solitary metal oxide.

A number of methods have been used to prepare mixed metal oxide materials including impregnation, selective grafting, chemical vapor deposition, mechanical mixing, coprecipitation, and solution sol−gel methods. The most important criteria to be obtained in these processes is homogeneity of the different components and control of the final metal-to-metal ratio. Combining the synthesis of binary metal oxide materials with the ability to maintain structural properties of large porosity and high specific surface area should give improved catalytic efficacy due to both the presence of a secondary metal oxide and structural control. Hence, templating procedures combined with the use of mixed alkoxide solutions are envisaged to attain this goal.

In this paper the formation of titania, zirconia, and the binary oxide (titania/zirconia) networks is accomplished using a templating process. The templating technique chosen makes use of already proven reliable polymer gel structures as templates,[17] and the sol−gel method, starting with infiltration of the precursor solutions within the polymer gel. The binary metal oxide materials are achieved by mixing the alkoxide solutions before infiltrating the solution into the polymer gel and then conducting hydrolysis and condensation reactions. These titania/zirconia systems were studied to obtain information on the structure−performance relationship in photocatalytic applications. To examine the photocatalytic efficiency of the titania and mixed materials, two prototype molecules, salicylic acid and 2-chlorophenol, have been studied. Salicylic acid, which chemisorbs to the titania surface via carboxylic groups,[18,19] has advantageous spectral characteristics allowing for the simple study of its decomposition, whereas chlorophenol is a chemical model for a number of the most dangerous water pollutants, especially in some third world countries. The degradation of the chlorophenol was studied by monitoring the concentration of the chloride ion formed during its degradation.

Table 1. Combinations of the Titania and Zirconia Precursors, Both per Gram of Initial Precursor Solution and per Mole, for the Preparation of Mixed Metal Oxide Networks

sample	TIP (g)	ZrP[a] (g)	2-PrOH (g)	Ti (mmol)	Zr (mmol)
M0	0.00	8.00	2.00	0.00	17.10
M10	0.50	7.41	1.98	1.76	15.83
M20	1.00	6.58	1.90	3.52	14.07
M30	1.50	5.76	1.81	5.28	12.31
M40	2.50	6.17	2.17	8.79	13.19
M50	3.00	4.94	1.98	10.55	10.55
M60	4.00	4.39	2.10	14.07	9.38
M70	5.00	3.53	2.13	17.58	7.54
M80	6.00	2.47	2.12	21.10	5.28
M90	7.00	1.28	2.07	24.62	2.74
M100	8.00	0.00	2.00	28.13	0.00

[a] Grams of ZrP precursor "as received"; dilution (70% in propanol) taken into consideration upon calculation of molar amount.

Experimental Section

Materials. For the production of the monolithic porous polymer templates, a well-established technique of polymerization in lyotropic surfactant phases was employed.[20−22] The surfactant Tween 60 (T60, polyoxyethylene (20) sorbitan monostearate), the monomers acrylamide (AA) and glycidyl methacrylate (GMA), ethylene glycol dimethacrylate as a cross-linker (EGDMA), and the initiator potassium persulfate (KPS) were purchased from Aldrich. The metal oxide precursors titanium(IV) isopropoxide (TIP, 99.999%) and zirconium(IV) propoxide (ZrP, 70% in propanol) were purchased from Aldrich and used as received. 2-Propanol (2-PrOH, 99.5%) was used for diluting the precursors and in the hydrolysis/condensation step with water. The water employed in all experiments was prepared in a three-stage Millipore Milli-Q Plus 185 purification system and had a resistivity higher than 18 MΩ cm.

The Degussa P25 titania sample supplied by Degussa-Hüls was measured to have a surface area of 45 $m^2\ g^{-1}$. It contains amorphous and crystalline titania, ≈80% of which is anatase and ≈20% has the rutile phase morphology.[23]

Polymer Gel Preparation. The porous polymer gel template was synthesized as follows: 25.00 g of the structure-directing surfactant, T60, was dissolved in 50.00 mL of water with stirring. After addition of the monomers (6.26 g of AA and 6.26 g of GMA) and cross-linker (2.51 g of EGDMA), stirring continued until a homogeneous, though turbid, solution was obtained. The initiator (0.63 g of KPS) was added and the solution transferred into test tubes that were then heated at 55 °C for 15 h in an oil bath, during which polymerization occurred. The gel was subsequently removed from the test tubes and cut into disks before being washed with water several times and then by Soxhlet extraction (ethanol, 2 days) to remove the surfactant. Further washing with water was performed until the conductivity of the washing solution no longer changed. This procedure gives a water and alcohol swellable gel with ≈70 vol % structural porosity.

Templating. The polymer gels were transferred via a slow solvent exchange procedure to 2-propanol, to ensure removal of water from the gel. The gels were then placed into precursor solutions (see Table 1) and soaked overnight (12−16 h). The precursor-filled gels were transferred to a water/2-propanol (1:1 vol) solution for hydrolysis and condensation reactions and left to soak overnight. After drying, the metal oxide/polymer hybrid was heated within 2 h to 500 °C under flowing nitrogen.

(10) Wilke, K.; Breuer, H. D. *J. Photochem. Photobiol. A: Chem.* **1999**, *121*, 49−53.
(11) Miller, J. B.; Edmond, I. K. *Catal. Today* **1997**, *35*, 269−292.
(12) Parida, K. M.; Samantaray, S. K.; Mishra, H. K. *J. Colloid Interface Sci.* **1999**, *216*, 127−133.
(13) Gao, X.; Wachs, I. E. *Catal. Today* **1999**, *51*, 233−254.
(14) Maity, S. K.; Rana, M. S.; Bej, S. K.; Ancheyta-Juárez, J.; Dhar, G. M.; Rao, T. S. R. P. *Catal. Lett.* **2001**, *72*, 115−119.
(15) Lai, S. Y.; Pan, W.; Ng, C. F. *Appl. Catal. B* **2000**, *24*, 207−217.
(16) Klimova, T.; Carmona, E.; Ramirez, J. *J. Mater. Sci.* **1998**, *33*, 1981−1990.
(17) Caruso, R. A.; Antonietti, M.; Giersig, M.; Hentze, H.-P.; Jia, J. *Chem. Mater.* **2001**, *13*, 1114−1123.
(18) Tunesi, S.; Anderson, M. *J. Phys. Chem.* **1991**, *95*, 3399−3405.
(19) Kratochvilova, K.; Hoskovcoca, I.; Jirkovsky, J.; Klima, J.; Ludvik, J. *Electrochim. Acta* **1995**, *40*, 2603−2609.
(20) Antonietti, M.; Hentze, H.-P. *Colloid Polym. Sci.* **1996**, *274*, 696−702.
(21) Antonietti, M.; Hentze, H.-P. *Adv. Mater.* **1996**, *8*, 840−844.
(22) Antonietti, M.; Caruso, R. A.; Göltner, C. G.; Weissenberger, M. C. *Macromolecules* **1999**, *32*, 1383−1389.
(23) Bickley, R. I.; Gonzalez-Carreno, T.; Lees, J. S.; Palmisano, L.; Tilley, R. J. D. *J. Solid State Chem.* **1991**, *92*, 178−190.

The samples were kept at this temperature for 10 h, during which the gas was changed to oxygen after the first hour.

The mixed metal oxide structures were formed by combining the titania and zirconia liquid precursors, which gave a homogeneous solution. The synthesis ratios of the samples discussed in this paper are given in Table 1.

Characterization. The structure of the materials produced (both polymeric and inorganic) was examined using scanning electron microscopy (SEM), Zeiss DSM 940 instrument. To prepare the samples for SEM investigation, the polymer gel was dried using a critical point drying technique (Critical Point Dryer, CPD 030 from BAL-TEC) after solvent exchange from water to ethanol and then to acetone (a method known to suppress drying artifacts[24]), and the inorganic networks were broken to expose fresh surfaces before mounting them onto carbon-coated stubs and sputter coating.

A Micromeritics Tristar instrument measured the specific surface area using BET (Brunauer−Emmett−Teller) analysis after N_2 sorption. Mercury intrusion porosimetry (MIP) was carried out at Micromeritics (Mönchengladbach, Germany) on a Micromeritics Mercury Porosimeter, AutoPoreIV, between the pressures of 0.0035 and 420 MPa. To determine the crystal phase of the inorganic materials produced, wide-angle X-ray scattering (WAXS), Enraf-Nonius PDS-120, was employed. A Netzsch TG 209 apparatus was used for thermogravimetric analysis, which gave the temperatures of total polymer pyrolysis and the weight percent of polymer to inorganic material in the intermediate stages.

Photocatalysis. *Salicylic Acid Photodecomposition.* UV−vis spectrometry (Agilent 8453 spectrophotometer) was used to monitor the absorbance spectra of salicylic acid as a function of illumination time. The salicylic acid (aqueous solution, 6 mL, 2.9×10^{-4} M) was stirred initially in the dark for 1.5 h in the presence of 0.015 g of inorganic material and then under illumination with a high-pressure mercury lamp, Marva 100 W, HBO 101/2. Light with wavelengths shorter than 350 nm was removed using a cutoff filter (WG-320, Schott). During illumination the solution was bubbled with air. The photocatalytic performance of the inorganic materials for the decomposition of salicylic acid was compared with a standard titanium dioxide sample, Degussa P25, which was also monitored under the same conditions.

2-Chlorophenol Photodecomposition. The photocatalytic activity of the prepared metal oxides was also tested in the decomposition reaction of 2-chlorophenol. The metal oxide networks were broken into small pieces that could be separated from solution using a 100-nm glass filter. The aqueous 2-chlorophenol solution (20 mL, 10^{-3} M, pH = 4.5) containing the photocatalyst (network or standard, Degussa P25) at a concentration of 2 g L^{-1} was stirred continuously while irradiating with a high-pressure mercury lamp (Philips HPK 125 W, total radiant flux was 10 mW cm^{-2}) equipped with IR−vis and UV filters for transmitting light within the range of $340 < \lambda < 500$ nm. An Orion chloride selective electrode was used for monitoring the chloride ion concentration, which gives a measure of the 2-chlorophenol decomposition.

Results and Discussion

The polymer template for forming the inorganic structure is opaque, spongelike, and homogeneous on a macroscopic scale. It can easily be handled with tweezers for transferral from different solutions. The porous structure of the polymer gel template could be observed after drying the polymer and breaking it to expose fresh surfaces and viewing on the SEM. As can be seen in Figure 1a, the polymer gel is homogeneously porous and has a globular structure. From mercury intrusion porosimetry (MIP) the pore sizes of the gel show a broad distribution around 1 μm (Figure 2). SEM images of the resulting inorganic materials (TiO_2 and ZrO_2) obtained from templating the polymer gel are also shown in Figure 1.

The structures show that a coating of the initial polymer was obtained, leaving a hollow globular material on removal of the polymer. On close inspection, minor amounts of inorganic material could be observed inside these hollow structures, indicating that the polymer gel is not only coated, but also the polymer itself was infiltrated to some extent by the precursor solutions (Figure 1d). An overall shrinkage (≈20%) can be observed when comparing the initial gel and the final inorganic structures, which is commonly seen after calcination of such materials.[6,7,17] MIP of the inorganic network gives a bimodal pore size distribution: The larger pores are those from the original polymer gel structure, which due to shrinkage during calcination and the additional thickness of the coated layer, are slightly smaller than those of the template (around 550 nm), whereas the smaller pores within the hollow replica structure are produced upon removal of the polymer scaffold. The wall thickness of the inorganic material is around 50 nm. (Control of the coating thickness can be obtained by variation of the precursor concentration and repetition of the coating cycles.[25]) The samples produced using mixed metal oxide precursors gave SEM images (data not shown) similar to those obtained for the individual zirconia and titania networks, which are displayed in Figure 1b−d.

X-ray analysis gave information about the crystal phase of the inorganic materials. Figure 3 shows the scattering curves of selected samples. The M100 network consists mainly of anatase titania crystals with traces of the rutile modification. The addition of 10 mol % zirconia stabilizes the anatase form, as the rutile phase could not be detected. A further increase of the zirconia content inhibits crystallization, as no crystallinity could be detected by X-ray in the binary metal oxide samples M80 to M40, thus indicating a homogeneous mixing of the Ti and Zr components in these materials. The scattering peaks from the samples containing zirconia as the major component, M30 to M0, can be assigned to either the monoclinic or tetragonal modification of zirconia.

The surface areas of these mixed TiO_2/ZrO_2 networks vary from 26 to 126 m^2 g^{-1}, as presented in Table 2, with the crystalline systems having lower surface areas than the amorphous ones. The presence of the second ion in sufficient amounts is obviously inhibiting crystallization and the consequent structural growth, resulting in higher surface areas.

The photodecomposition of salicylic acid was studied by monitoring the absorbance of the salicylic acid solution at the absorption maximum (wavelength of 296 nm) of the aromatic acid and has been plotted in Figure 4. Two interesting pieces of information can be obtained from these data: First, the rate of decomposition with illumination time (available from the slope of the curves) and second the comparative adsorbent properties of the mixed metal oxide networks (which is related to the ordinate intercept). The reference (i.e., the Degussa P25 titania sample) shows the most efficient catalytic prop-

(24) Reimer, L.; Pfefferkorn, G. *Scanning Electron Microscopy*; Springer: Berlin, 1972.

(25) Schattka, J. H.; Antonietti, M.; Caruso, R. A. In preparation.

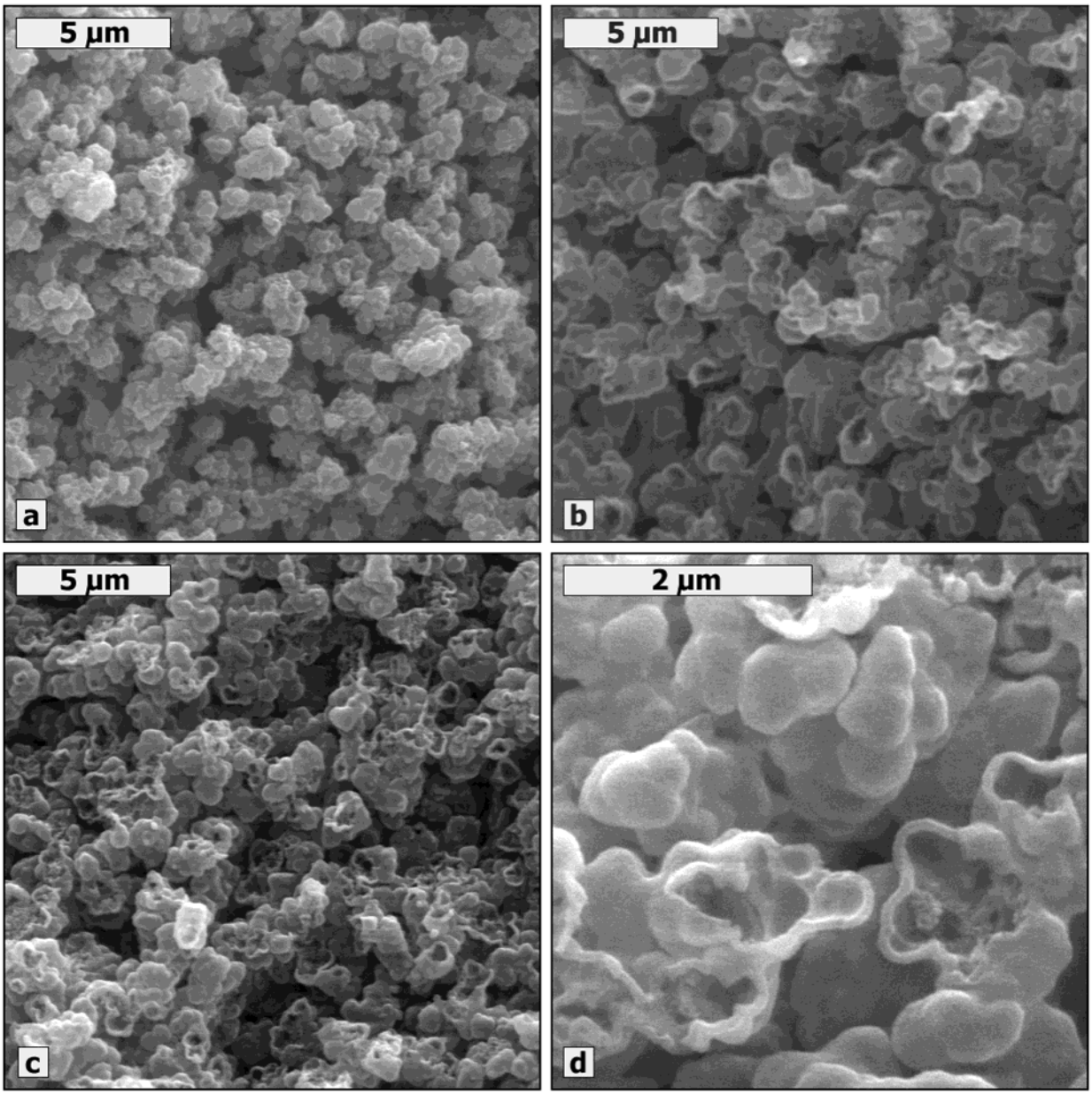

Figure 1. SEM images of (a) the initial polymer gel template, (b) the ZrO_2 network (M0), and (c) and d) the TiO_2 network (M100) at different magnifications.

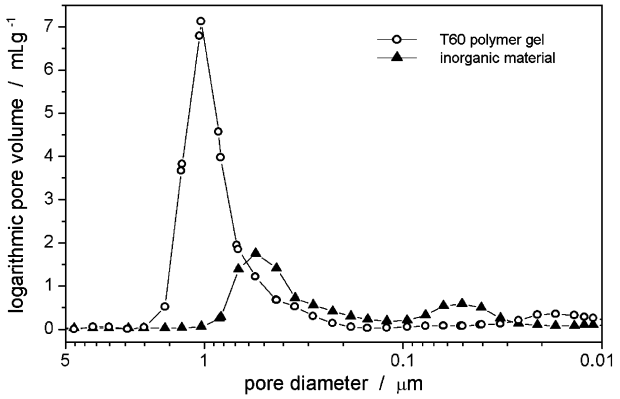

Figure 2. Mercury intrusion results for the polymer gel template and the titania/zirconia material (M50).

erties for this reaction. It must be kept in mind that this comparison is biased, since Degussa P25 consists of highly dispersed nanoparticles (with a surface area of 45 $m^2\ g^{-1}$) that show no diffusion or transport limitation, but make its employment in a simple reaction device difficult due to separation problems.

The titania network, M100, has an efficiency of ≈60% that of Degussa P25. The surface area of this sample is 31 $m^2\ g^{-1}$, about 69% the surface area of Degussa P25, and it is composed primarily of anatase crystals. In the case of the network samples, the materials were broken into smaller pieces for testing the catalytic reaction. The lower surface area, the different crystal composition, and the catalyst morphology all contribute to the altered catalytic performance.

For the mixed titania/zirconia networks the catalytic activities of the materials are seen to decrease with an increase in the amount of zirconia present (M90−M0). This decrease in activity is not surprising when the following points are taken into consideration: First, zirconia has a very large band gap, greater than 5 eV,[26] so it cannot act as a photocatalyst under the irradiation

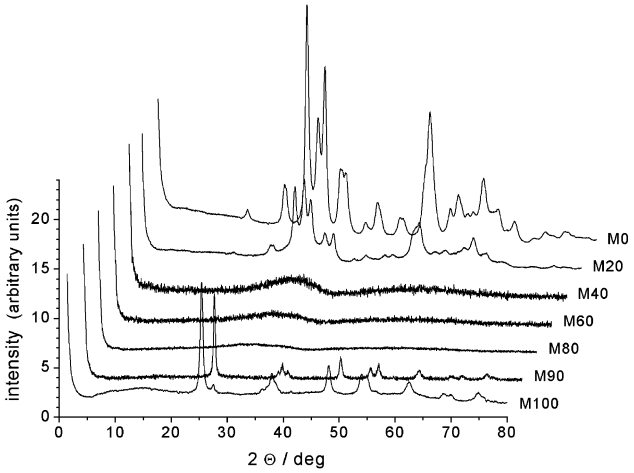

Figure 3. Wide-angle X-ray scattering curves for the mixed TiO_2/ZrO_2 networks.

Table 2. BET Surface Areas (SA) Obtained from Nitrogen Adsorption Measurements and the Crystal Modifications Determined from WAXS for the Mixed Titania/Zirconia Networks[a]

sample	SA ($m^2\ g^{-1}$)	crystal modification
M0	48	m-ZrO_2, t-ZrO_2
M10	26	m-ZrO_2, t-ZrO_2
M20	47	m-ZrO_2, t-ZrO_2
M30	87	m-ZrO_2, t-ZrO_2
M40	109	(amorph)
M50	121	(amorph)
M60	127	(amorph)
M70	126	(amorph)
M80	100	(amorph)
M90	43	A
M100	31	A, traces of R

[a] Abbreviations: m, monoclinic; t, tetragonal; A, anatase; R, rutile; amorph, no peaks obtained in WAXS, indicating amorphous material.

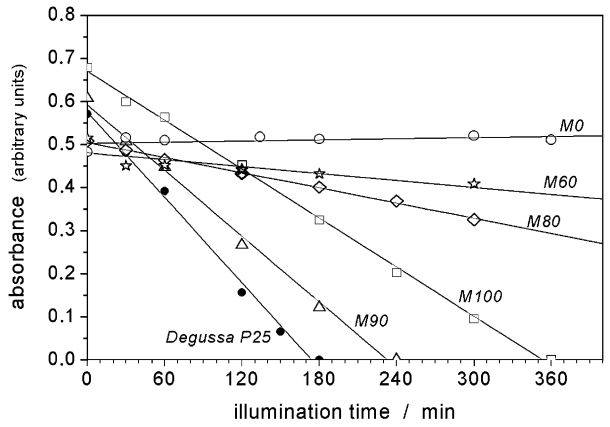

Figure 4. Salicylic acid photodecomposition for the Degussa P25 standard and the mixed TiO_2/ZrO_2 networks with various Ti/Zr ratios plotted as the salicylic acid absorbance at a wavelength of 296 nm as a function of illumination time.

conditions used for these experiments. Second, the WAXS measurements for the samples M80−M0 do not show peaks corresponding to crystalline titania, and amorphous titania is known to have negligible photocatalytic efficiency compared to that of the anatase or rutile phase, due to an increased rate of electron/hole recombination.[27] In addition, salicylic acid forms a complex with the surface of the anatase crystal,[18,19] which facilitates the hole transfer. So, in the absence of the anatase phase and hence surface complexation, the decomposition has to proceed via the less direct route of the generated intermediates (˙OH radicals). The presence of some activity for the M80 sample would suggest either the presence of crystalline titania, which could not be detected using our WAXS apparatus, or that the mixed titania/zirconia glass had photocatalytic activity.

Interestingly, the efficiency of the M90 sample is about 80% that of Degussa P25; that is, it is more efficient than the pure titania sample. This sample has a surface area of 43 $m^2\ g^{-1}$ (96% that of P25 and 140% that of M100) and consists of the anatase crystalline phase of titania. A number of factors could be contributing to this increased efficiency compared to that of the pure titania network: (i) The M90 sample has a larger surface area, (ii) anatase is believed to be more photocatalytically active than the rutile phase[28] and the addition of a second metal oxide to titania is known to inhibit the anatase-to-rutile phase transformation,[29] and (iii) zirconia is known to be a good adsorbent.[30,31]

The last argument is also experimentally supported when comparing the adsorption strength of the samples in Figure 4: the lower the UV absorption at zero time, the more salicylic acid is adsorbed to the particles. The absolute value of the absorbance after soaking in the dark can be seen to decrease as the zirconia content of the sample increases (M100−M80), indicating an increased adsorption of salicylic acid on the catalyst during the 1.5 h of catalyst/salicylic acid interaction in the dark. Increased adsorbance of the salicylic acid on the catalyst surface enhances the probability of a potential catalytic reaction due to the close proximity of the molecule with the titania surface and the oxidizing radicals (˙OH) formed on illumination of the titania material.

Figure 5 shows the photodecomposition of 2-chlorophenol, monitored by the chloride ion concentration as a function of illumination time of the Degussa P25 titania, and the TiO_2 (M100) and TiO_2/ZrO_2 (M70−M90) networks. The photocatalytic activity of the pure titania network for this reaction is lower than that of the reference material, with about 65% comparative efficiency. As for the salicylic acid photodecomposition, the activity is increased considerably by the addition of 10% zirconia, resulting in similar efficiencies to the Degussa P25. However, in contrast to the previous photocatalytic reaction, there is a less pronounced drop in proficiency for the samples containing higher contents of zirconia, M80 and M70, although they did not show evidence of crystallinity (WAXS). 2-Chlorophenol does not form complexes with the crystalline surface of the catalyst,[32] and the oxidation reaction proceeds via the intermedi-

(26) Nozik, A. J. *Annu. Rev. Phys. Chem.* **1978**, *29*, 189−222.
(27) Ohtani, B.; Ogawa, Y.; Nishimoto, S. *J. Phys. Chem. B* **1997**, *101*, 3746−3752.
(28) Hoffmann, M. R.; Martin, S. T.; Choi, W.; Bahnemann, D. W. *Chem. Rev.* **1995**, *95*, 69−96.
(29) Poznyak, S. K.; Kokorin, A. I.; Kulak, A. I. *J. Electroanal. Chem.* **1998**, *442*, 99−105.
(30) Dobson, K. D.; McQuillan, A. J. *Spectrochim. Acta* **2000**, *56*, 557−565.
(31) Fu, X.; Clark, L. A.; Yang, Q.; Anderson, M. A. *Environ. Sci. Technol.* **1996**, *30*, 647−653.
(32) Ku Y.; Leu R.-M.; Lee K.-C. *Water Res.* **1996**, *30*, 2569−2578.

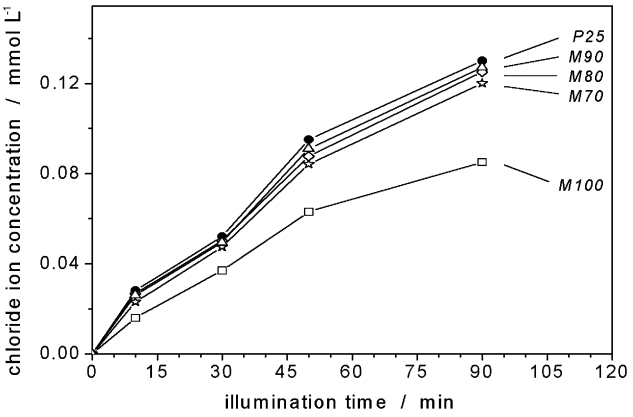

Figure 5. Photodecomposition of 2-chlorophenol for the Degussa P25 standard and the mixed TiO_2/ZrO_2 networks with various Ti/Zr ratios plotted as the chloride ion concentration as a function of illumination time.

ates (·OH radicals) generated. Hence, the lack of crystalline surface is not a significant hindrance in this system. As the amorphous titania is not expected to be producing ·OH radicals, this again suggests that either the amorphous binary (TiO_2/ZrO_2) material has photocatalytic activity or there is sufficient undetected crystalline material for this to be compensated.

Conclusions

Templating of macroporous polymer gels with mixed sol−gel precursor solutions leads to the generation of monolithic macroporous networks, with two different pore systems and a high pore connectivity. Depending on the metal ratios, different crystalline and amorphous oxidic phases were obtained. It was shown that the addition of zirconia to the titania significantly increased the surface area compared to that of the pure titania material. While small amounts (10%) of zirconia stabilized the anatase phase of the titania, crystallization of the metal oxides was not detectable for larger (20−60%) zirconia contents.

These systems were assessed for application as catalysts in two photodecomposition reactions. Compared to the pure titania material, the catalytic efficiency was increased by the addition of 10% zirconia for both the salicylic acid and 2-chlorophenol decomposition. This was attributed to several factors including the increased surface area of the material, the crystal phase of the titania, and the adsorptive properties of the zirconia, which is believed to increase the local concentration of the reactant near the catalyst surface.

The loss of crystallinity with increased zirconia content leads to a decrease in activity, which is more pronounced for the salicylic acid decomposition. This was explained by the complex formation of the salicylic acid with the anatase crystal surface, which promoted its decomposition. The oxidation of 2-chlorophenol, which does not form such complexes, is influenced less by the lack of crystallinity.

Therefore, the combination of binary metal oxide material synthesis with the polymer gel templating technique can lead to interesting catalysts with an otherwise nonaccessible combination of properties, such as excellent transport behavior, large porosity, and high specific surface area, which result in improved catalytic performance.

Acknowledgment. Degussa Hüls is thanked for donating the Degussa P25 nanoparticles. The Max Planck Society is acknowledged for financial support, and D.G.S. is grateful to the German Academic Exchange Service, DAAD, for a 1-year scholarship (No. A/01/10817).

CM021238K